

An Importance Sampling Scheme on Dual Factor Graphs. II. Models with Strong Couplings

Mehdi Molkaraie

mehdi.molkaraie@alumni.ethz.ch

Abstract—We consider the problem of estimating the partition function of the two-dimensional ferromagnetic Ising and Potts models in an external magnetic field. The estimation is done via importance sampling in the dual of the Forney factor graph representing the models. We present importance sampling schemes that can efficiently compute an estimate of the partition function in a wide range of model parameters. Emphasis is on models in which a subset of the coupling parameters is strong.

I. INTRODUCTION

We consider the problem of computing the partition function of the finite-size two-dimensional (2D) ferromagnetic Ising model in an external magnetic field. Applying factor graph duality to address the problem has been investigated in [1]–[3]. It was demonstrated in [1] that Monte Carlo methods based on the dual factor graph work very well for the Ising model at low temperature. In contrast, Monte Carlo methods in the original graph, suffer from critical slowing down at low temperature [4]. Monte Carlo methods in the dual factor graph were also proposed in [1] to estimate the partition function of 2D Ising models in the absence of an external field. In [2], an importance sampling scheme was proposed on the dual factor graph to compute the partition function of the 2D Ising model and the 2D Potts model, when the models are under the influence of an external magnetic field. The importance sampling scheme of [2] was specifically designed for models that are in a strong external field.

In the present paper, we continue this investigation to extend the results of [1], [2] to models with a mixture of strong and weak coupling parameters, and show that in order to have efficient Monte Carlo methods in the dual factor graph, not all the coupling parameters need to be strong (corresponding to models at low temperature), but only a restricted subset of them. As in [2], the proposed importance sampling schemes operate in the dual of the Forney factor graph representing the model. Our numerical results show that the schemes can efficiently estimate the partition function in a wide range of model parameters.

In our schemes, samples are drawn in the dual domain, therefore, as was pointed out in [2], the proposed schemes do not suggest a direct method to draw samples according to the Boltzmann distribution. For more details, see [5, Section II.2], [6], [7].

The paper is organized as follows. In Section II, we review the Ising model and its graphical model representation in terms of Forney factor graphs. Section III discusses dual Forney factor graphs and the normal factor graph duality theorem.

Sections II and III mainly follow the introductory sections of [2]. Section IV describes the proposed importance sampling schemes and the corresponding algorithms. Generalizations to the q -state Potts model are briefly discussed in Section V. Numerical experiments are reported in Section VI.

II. THE ISING MODEL IN AN EXTERNAL MAGNETIC FIELD

Let X_1, X_2, \dots, X_N be a collection of discrete random variables arranged on the sites of a 2D lattice, as illustrated in Fig. 1, where interactions are restricted to adjacent (nearest-neighbor) variables. Suppose each random variable takes on values in some finite alphabet \mathcal{X} . Let x_i represent a possible realization of X_i , \mathbf{x} stand for a configuration (x_1, x_2, \dots, x_N) , and let \mathbf{X} stand for (X_1, X_2, \dots, X_N) .

In a 2D Ising model (a.k.a. Lenz-Ising model, see [8] for an introduction and [9] for a historical review), $\mathcal{X} = \{0, 1\}$ and the energy of a configuration \mathbf{x} is given by the Hamiltonian [10]

$$\mathcal{H}(\mathbf{x}) = - \sum_{(k, \ell) \in \mathcal{B}} J_{k, \ell} \cdot ([x_k = x_\ell] - [x_k \neq x_\ell]) - \sum_{m=1}^N H_m \cdot ([x_m = 1] - [x_m = 0]) \quad (1)$$

where \mathcal{B} contains all the pairs (bonds) (k, ℓ) with non-zero interactions, and $[\cdot]$ denotes the Iverson bracket [11], which evaluates to 1 if the condition in the bracket is satisfied and to 0 otherwise.

The real coupling parameter $J_{k, \ell}$ controls the strength of the interaction between adjacent variables (x_k, x_ℓ) . The real parameter H_m corresponds to the presence of an external magnetic field and controls the strength of the interaction between X_m and the field.

In this paper, the focus is on ferromagnetic Ising models characterized by $J_{k, \ell} > 0$, for each $(k, \ell) \in \mathcal{B}$. In ferromagnetic Ising models, configurations in which adjacent variables take the same values, have low energy levels.

In thermal equilibrium, the probability that the model is in configuration \mathbf{x} , is given by the Boltzmann distribution

$$p_{\mathbf{B}}(\mathbf{x}) \triangleq \frac{e^{-\beta \mathcal{H}(\mathbf{x})}}{Z} \quad (2)$$

Here, Z is the partition function (the normalization constant) $Z = \sum_{\mathbf{x} \in \mathcal{X}^N} e^{-\beta \mathcal{H}(\mathbf{x})}$ and $\beta \triangleq \frac{1}{k_{\text{B}} T}$, where T denotes the temperature and k_{B} is Boltzmann's constant [10].

The Helmholtz free energy is defined as

$$F_H \triangleq -\frac{1}{\beta} \ln Z \quad (3)$$

The Helmholtz free energy is an important quantity in statistical physics as all macroscopic thermodynamic properties of a model follow from differentiating F_H (as a function of the temperature); see [10, Chapter 2]. In the rest of this paper, we assume $\beta = 1$.

For each adjacent pair (x_k, x_ℓ) , let

$$\kappa_{k,\ell}(x_k, x_\ell) = e^{J_{k,\ell} \cdot ([x_k=x_\ell] - [x_k \neq x_\ell])} \quad (4)$$

and for each x_m

$$\tau_m(x_m) = e^{H_m \cdot ([x_m=1] - [x_m=0])} \quad (5)$$

We can then define $f : \mathcal{X}^N \rightarrow \mathbb{R}_{>0}$ as

$$f(\mathbf{x}) \triangleq \prod_{(k,\ell) \in \mathcal{B}} \kappa_{k,\ell}(x_k, x_\ell) \prod_{m=1}^N \tau_m(x_m) \quad (6)$$

The corresponding Forney factor graph (normal graph) for the factorization in (6) is shown in Fig. 1, where the boxes labeled “=” are equality constraints [12], [13]. In Forney factor graphs variables are represented by edges.

From (6), Z in (2) can be expressed as

$$Z = \sum_{\mathbf{x} \in \mathcal{X}^N} f(\mathbf{x}) \quad (7)$$

At high temperature (i.e., small J), the Boltzmann distribution (2) approaches the uniform distribution. Therefore, to estimate Z and other quantities of interest (e.g., the mean magnetization), Monte Carlo methods in the original graph usually perform well [4], [14], [15].

In this paper, we consider a curious case where a restricted subset of the coupling parameters of the model is strong (i.e., large J). To compute an estimate of Z in this case, we propose importance sampling schemes that operates in the dual of the Forney factor graph representing the factorization in (6).

III. THE DUAL MODEL

We can obtain the dual of the Forney factor graph in Fig. 1, by replacing each variable x with its dual variable \tilde{x} , each factor $\kappa_{k,\ell}$ with its 2D Discrete Fourier transform (DFT), each factor τ_m with its one-dimensional (1D) DFT, and each equality constraint with an XOR factor, cf. [12], [16]–[18]. Note that, \tilde{X} also takes on values in \mathcal{X} .

After suitable modifications, we can construct the (modified) dual Forney factor graph as in Fig. 2, with XOR factors as

$$g(\tilde{x}_1, \tilde{x}_2, \dots, \tilde{x}_k) = [\tilde{x}_1 \oplus \tilde{x}_2 \oplus \dots \oplus \tilde{x}_k = 0] \quad (8)$$

where \oplus denotes the sum in GF(2), with factors attached to each XOR factor as

$$\lambda_m(\tilde{x}_m) = \begin{cases} 2 \cosh H_m, & \text{if } \tilde{x}_m = 0 \\ -2 \sinh H_m, & \text{if } \tilde{x}_m = 1 \end{cases} \quad (9)$$

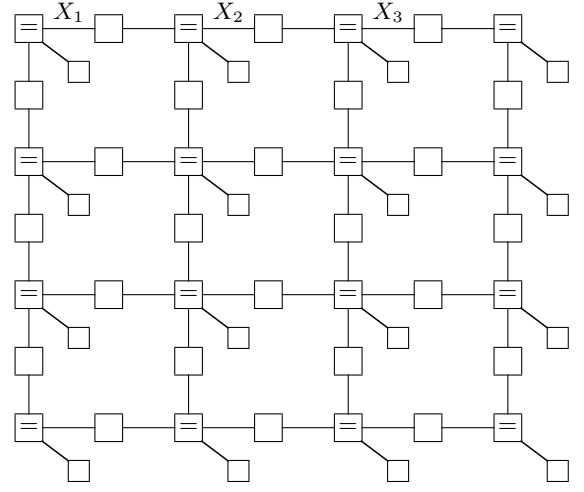


Fig. 1. Forney factor graph of a 2D Ising model in an external field, where the unlabeled normal-size boxes represent factors as in (4), the small boxes represent factors as in (5), and the boxes containing “=” symbols are equality constraints.

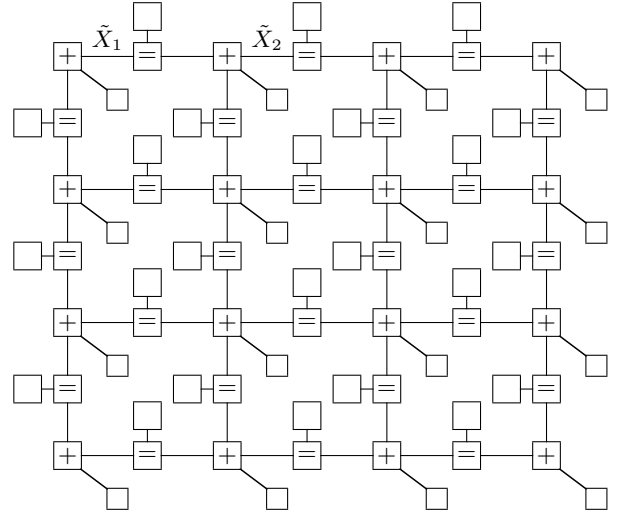


Fig. 2. The dual Forney factor graph of a 2D Ising model in an external field, where the small boxes represent factors as in (9), the unlabeled normal-size boxes represent factors as in (10), and boxes containing “+” symbols represent XOR factors as in (8).

and with factors attached to each equality constraint as

$$\gamma_k(\tilde{x}_k) = \begin{cases} 4 \cosh J_k, & \text{if } \tilde{x}_k = 0 \\ 4 \sinh J_k, & \text{if } \tilde{x}_k = 1 \end{cases} \quad (10)$$

Here, J_k is the coupling parameter associated with each bond (the bond strength). For more details on constructing the dual factor graph of the 2D Ising and Potts models, see [1]–[3].

In the dual domain, we denote the partition function by Z_d and the number of edges by E . For the models that we study here, the normal factor graph duality theorem states that

$$Z_d = |\mathcal{X}^E| Z \quad (11)$$

see [16], [17, Theorem 2].

In this paper, the focus is on ferromagnetic models, therefore all the factors as in (10) are positive. Since in a 2D Ising

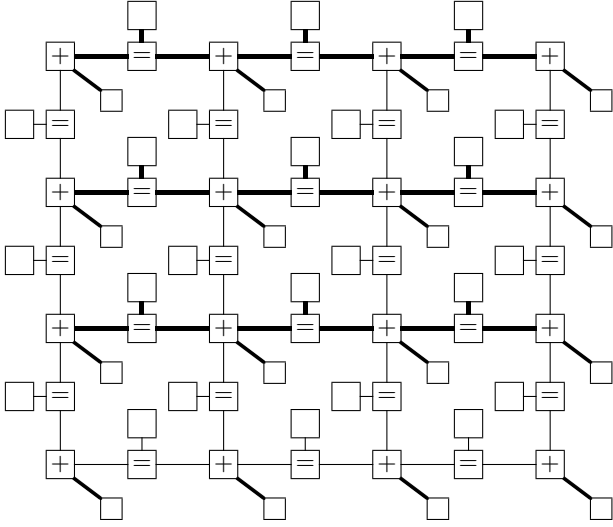


Fig. 3. The partitioning of variables on the dual Forney factor graph used in Algorithm 1. The thick edges represent variables in $\tilde{\mathbf{X}}_A$, and the remaining edges represent variables in $\tilde{\mathbf{X}}_B$.

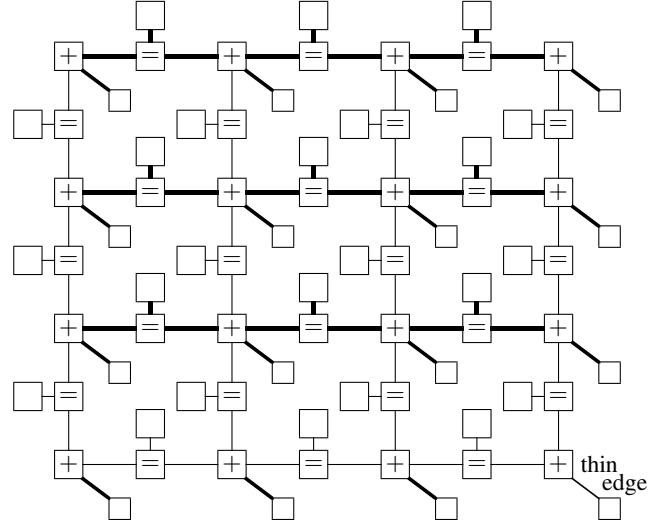


Fig. 4. The partitioning of variables on the dual Forney factor graph used in Algorithm 2. The thick edges represent variables in $\tilde{\mathbf{X}}_A$, and the remaining edges represent variables in $\tilde{\mathbf{X}}_B$.

model, the value of Z is invariant under the change of sign of the external field [19], without loss of generality, we assume $H_m < 0$. With this assumption, all the factors as in (9) will also be positive. In Section IV, we use the dual representation of the 2D Ising model to give an alternative proof for the invariance of Z under the change of sign of the external field.

IV. IMPORTANCE SAMPLING SCHEMES ON THE DUAL FACTOR GRAPH

In this section, we propose two importance sampling schemes in the dual Forney factor graph to compute an estimate of Z , as in (7). Our importance sampling schemes operate in the dual Forney factor graph of the 2D Ising model in an external magnetic field, see Fig. 2.

As in [1], [2], we partition the set of random variables $\tilde{\mathbf{X}}$, into $\tilde{\mathbf{X}}_A$ and $\tilde{\mathbf{X}}_B$, with the condition that the random variables in $\tilde{\mathbf{X}}_B$ are linear combinations (involving the XOR factors) of the random variables in $\tilde{\mathbf{X}}_A$. Note that, a valid configuration in the dual graph can be generated by assigning values to $\tilde{\mathbf{X}}_A$, followed by computing $\tilde{\mathbf{X}}_B$ as linear combinations of $\tilde{\mathbf{X}}_A$.

Two examples of such a partitioning are illustrated in Figs. 3 and 4, where we let $\tilde{\mathbf{X}}_A$ be the set of all the variables associated with the thick edges, and $\tilde{\mathbf{X}}_B$ the set of all the variables associated with the remaining thin edges. Accordingly, we let \mathcal{B}_A , a subset of \mathcal{B} , contain all the indices of the bonds marked by the thick edges, and $\mathcal{B}_B = \mathcal{B} - \mathcal{B}_A$.

For a valid configuration $\tilde{\mathbf{x}} = (\tilde{\mathbf{x}}_A, \tilde{\mathbf{x}}_B)$, suppose $\tilde{\mathbf{x}}_A = (\tilde{\mathbf{y}}, \tilde{\mathbf{z}})$, where $\tilde{\mathbf{y}}$ contains all the thick edges attached to the small unlabeled boxes, which represent variables that are involved in factors as in (9), and $\tilde{\mathbf{z}}$ contains all the variables associated with the thick bonds.

We show that $w_H(\tilde{\mathbf{y}})$, the Hamming weight of $\tilde{\mathbf{y}}$, is always even, where the Hamming weight of a vector is the number of non-zero components of that vector [20].

Lemma 1. If $\tilde{\mathbf{x}}$ is a valid configuration in the dual Forney factor graph of the 2D Ising model, then $w_H(\tilde{\mathbf{y}})$ is even.

Proof. We consider c , the component-wise XOR of $\tilde{\mathbf{y}}$, as $c = \bigoplus_{m=1}^N \tilde{y}_m$. Each XOR factor imposes the constraint that all its incident variables sum to 0 in $\text{GF}(2)$. In c , each \tilde{y}_m can thus be expanded as the XOR of the corresponding variables associated with the bonds, furthermore, the variables on the bonds each appears twice in this expansion. We conclude that $c = 0$, i.e., $w_H(\tilde{\mathbf{y}})$ is even. ■

In Lemma 1, the choice of the boundary conditions (free or periodic) is immaterial. Lemma 1 implies that the value of Z_d , and equivalently the value of Z , are invariant under the change of sign of the external magnetic field. Indeed, regardless of the sign of the external field H_m , i.e., assigned to all positive or to all negative values, $\prod_{m=1}^N \lambda_m(\tilde{x}_m)$ takes on the same positive value, see (9).

In the following, we present two slightly different algorithms for estimating the partition function. Both algorithms use importance sampling and follow the same procedure: to draw $\tilde{\mathbf{x}}^{(\ell)}$ at each iteration ℓ , we first draw a sample $\tilde{\mathbf{x}}_A^{(\ell)}$ according to a suitably defined auxiliary probability mass function, we then update $\tilde{\mathbf{x}}_B^{(\ell)}$ in order to generate $\tilde{\mathbf{x}}^{(\ell)} = (\tilde{\mathbf{x}}_A^{(\ell)}, \tilde{\mathbf{x}}_B^{(\ell)})$. Since $\tilde{\mathbf{x}}_B$ is a linear combination of $\tilde{\mathbf{x}}_A$, at each iteration, $\tilde{\mathbf{x}}_B^{(\ell)}$ can be updated in a straightforward manner.

A. Algorithm 1

The partitioning used in Algorithm 1 is illustrated in Fig. 3. Hence, $\tilde{\mathbf{X}}_A$ contains all the variables associated with the edges attached to the small unlabeled boxes, which are involved in factors as in (9), as well as all the variables associated with the thick bonds, which are involved in factors as in (10).

Let us define

$$\Lambda_1(\tilde{\mathbf{X}}_B) \triangleq \prod_{k \in \mathcal{B}_B} \gamma_k(\tilde{X}_k) \quad (12)$$

$$\Psi_1(\tilde{\mathbf{X}}_A) \triangleq \prod_{k \in \mathcal{B}_A} \gamma_k(\tilde{X}_k) \prod_{m=1}^N \lambda_m(\tilde{X}_m) \quad (13)$$

We use the following probability mass function as the auxiliary distribution in our importance sampling scheme

$$q_1(\tilde{\mathbf{x}}_A) \triangleq \frac{\Psi_1(\tilde{\mathbf{x}}_A)}{Z_{q_1}} \quad (14)$$

The partition function Z_{q_1} , is analytically available as

$$Z_{q_1} = \sum_{\tilde{\mathbf{x}}_A} \Psi_1(\tilde{\mathbf{x}}_A) \quad (15)$$

$$= 2^{N+2|\mathcal{B}_A|} \exp\left(\sum_{k=1}^{|\mathcal{B}_A|} J_k - \sum_{m=1}^N H_m\right) \quad (16)$$

where $|\mathcal{B}_A|$ is the cardinality of \mathcal{B}_A . Note that $H_m < 0$.

The product form of (13) suggests that at each iteration ℓ , to draw a sample $\tilde{\mathbf{x}}_A^{(\ell)} = (\tilde{\mathbf{y}}^{(\ell)}, \tilde{\mathbf{z}}^{(\ell)})$ according to $q_1(\tilde{\mathbf{x}}_A)$, two separate subroutines are required, one to draw the $\tilde{\mathbf{y}}^{(\ell)}$ -part, and the other to draw the $\tilde{\mathbf{z}}^{(\ell)}$ -part.

To draw the $\tilde{\mathbf{y}}^{(\ell)}$ -part, we apply the following subroutine.

repeat

draw $u_1^{(\ell)}, u_2^{(\ell)}, \dots, u_N^{(\ell)} \stackrel{\text{i.i.d.}}{\sim} \mathcal{U}[0, 1]$

for $m = 1$ **to** N

if $u_m^{(\ell)} < \frac{1}{2}(1 + e^{2H_m})$

$\tilde{y}_m^{(\ell)} = 0$

else

$\tilde{y}_m^{(\ell)} = 1$

end if

end for

until $w_H(\tilde{\mathbf{y}}^{(\ell)})$ is even

The criteria to accept $\tilde{\mathbf{y}}^{(\ell)}$ is based on Lemma 1. The quantity $\frac{1}{2}(1 + e^{2H_m})$ is equal to $\lambda_m(0)/(\lambda_m(0) + \lambda_m(1))$.

To draw the $\tilde{\mathbf{z}}^{(\ell)}$ -part, the following subroutine is applied.

draw $u_1^{(\ell)}, u_2^{(\ell)}, \dots, u_{|\mathcal{B}_A|}^{(\ell)} \stackrel{\text{i.i.d.}}{\sim} \mathcal{U}[0, 1]$

for $k = 1$ **to** $|\mathcal{B}_A|$

if $u_k^{(\ell)} < \frac{1}{2}(1 + e^{-2J_k})$

$\tilde{z}_k^{(\ell)} = 0$

else

$\tilde{z}_k^{(\ell)} = 1$

end if

end for

Here, $\frac{1}{2}(1 + e^{-2J_k})$ is equal to $\gamma_k(0)/(\gamma_k(0) + \gamma_k(1))$. We can then generate $\tilde{\mathbf{x}}_A^{(\ell)}$ as a concatenation of $\tilde{\mathbf{y}}^{(\ell)}$ and $\tilde{\mathbf{z}}^{(\ell)}$, in any predetermined order.

B. Algorithm 2

One can design an algorithm with no rejections by adopting a different choice of partitioning on the dual graph, as depicted in Fig. 4. The only difference between the partitionings in Figs. 3 and 4, is that in Fig. 4 one of the edges attached to the small unlabeled boxes (indicated by “thin edge”) is excluded from $\tilde{\mathbf{X}}_A$. For simplicity, let us assume that the excluded edge (variable) is involved in $\lambda_N(\cdot)$.

We thus define

$$\Lambda_2(\tilde{\mathbf{X}}_B) \triangleq \lambda_N(\tilde{X}_N) \prod_{k \in \mathcal{B}_B} \gamma_k(\tilde{X}_k) \quad (17)$$

$$\Psi_2(\tilde{\mathbf{X}}_A) \triangleq \prod_{k \in \mathcal{B}_A} \gamma_k(\tilde{X}_k) \prod_{m=1}^{N-1} \lambda_m(\tilde{X}_m) \quad (18)$$

Similarly, the auxiliary distribution $q_2(\tilde{\mathbf{x}}_A)$ is as

$$q_2(\tilde{\mathbf{x}}_A) \triangleq \frac{\Psi_2(\tilde{\mathbf{x}}_A)}{Z_{q_2}} \quad (19)$$

where Z_{q_2} is also analytically available.

Again, the product form of (18) suggests that at each iteration ℓ , two separate subroutines are required to draw $\tilde{\mathbf{x}}_A^{(\ell)} = (\tilde{\mathbf{y}}^{(\ell)}, \tilde{\mathbf{z}}^{(\ell)})$ according to $q_2(\tilde{\mathbf{x}}_A)$.

To draw the $\tilde{\mathbf{y}}^{(\ell)}$ -part, we apply the following subroutine, which has no rejections.

draw $u_1^{(\ell)}, u_2^{(\ell)}, \dots, u_{N-1}^{(\ell)} \stackrel{\text{i.i.d.}}{\sim} \mathcal{U}[0, 1]$

for $m = 1$ **to** $N - 1$

if $u_m^{(\ell)} < \frac{1}{2}(1 + e^{2H_m})$

$\tilde{y}_m^{(\ell)} = 0$

else

$\tilde{y}_m^{(\ell)} = 1$

end if

end for

set $\tilde{y}_N^{(\ell)} = \bigoplus_{m=1}^{N-1} \tilde{y}_m^{(\ell)}$

Drawing the $\tilde{\mathbf{z}}^{(\ell)}$ -part can be treated in an analogous way as in Algorithm 1 (with the same subroutine). After this, we can generate $\tilde{\mathbf{x}}_A^{(\ell)}$ from $\tilde{\mathbf{y}}^{(\ell)}$ and $\tilde{\mathbf{z}}^{(\ell)}$.

C. Estimating Z

Each of two algorithms will provide independent samples $\tilde{\mathbf{x}}_A^{(1)}, \tilde{\mathbf{x}}_A^{(2)}, \dots, \tilde{\mathbf{x}}_A^{(\ell)}, \dots$ according to its auxiliary distribution. As previously mentioned, after generating $\tilde{\mathbf{x}}_A^{(\ell)}$, updating $\tilde{\mathbf{x}}_B^{(\ell)}$ is easy. The samples are then used in the following importance sampling scheme to estimate Z_d/Z_q ,

for $\ell = 1$ **to** L

draw $\mathbf{x}_A^{(\ell)}$ according to $q(\tilde{\mathbf{x}}_A)$

update $\tilde{\mathbf{x}}_B^{(\ell)}$

end for

compute

$$\hat{r}_{\text{IS}} = \frac{1}{L} \sum_{\ell=1}^L \Lambda(\tilde{\mathbf{x}}_B^{(\ell)}) \quad (20)$$

Here, $q(\cdot)$ and $\Lambda(\cdot)$ are selected in accordance with the applied algorithm (Algorithm 1 or Algorithm 2), and Z_q denotes the corresponding partition function.

It follows that \hat{r}_{IS} is an unbiased (and consistent) estimator of Z_d/Z_q . Indeed

$$\mathbb{E}[\hat{r}_{\text{IS}}] = \frac{Z_d}{Z_q} \quad (21)$$

Since Z_q is analytically available, the proposed importance sampling scheme can yield an estimate of Z_d , which can then be used to estimate Z in (7), using the normal factor graph duality theorem, cf. Section III.

The accuracy of the estimator (20) depends on the fluctuations of $\Lambda(\tilde{\mathbf{x}}_B)$. If $\Lambda(\tilde{\mathbf{x}}_B)$ varies smoothly, \hat{r}_{IS} will have a small variance. From (12), we expect to observe a small variance in Algorithm 1 if for each $k \in \mathcal{B}_B$, J_k is large. With the exception of one factor, similar behavior is expected in Algorithm 2, see Section VI-D.

A few comments on the proposed schemes are in order.

- A good strategy in Algorithm 2 is therefore to exclude a variable (an edge) involved in a factor with a large H_m , see (17). We will apply this strategy in the numerical experiments of Section VI-A.
 - We emphasize that our choices of partitioning in Figs. 3 and 4 are not unique. Fig. 5 shows another example of a partitioning on the dual factor graph. Moreover, model parameters and their spatial distributions suggest which choices are expected to perform better in practice. E.g., a suitable partitioning for models in a strong external field is discussed in [2].
 - The proposed schemes are applicable to the Ising model in the absence of an external magnetic field as well. E.g., partitionings in Figs. 3 to 5 are valid even if the external field is not present. We will consider Ising models in the absence of an external field in our numerical experiments in Section VI-B.
- That being the case, to observe fast convergence in the dual domain, not all the coupling parameters need to be strong, but a restricted subset of them. Therefore, the schemes of this paper can be regarded as supplementary to the schemes presented in [1], where the focus was on models at low temperature (corresponding to models in which all the coupling parameters are strong).
- If a restricted subset of the coupling parameters is relatively strong, ideas from annealed importance sampling [21]–[23] can be employed, see Appendix I.

V. GENERALIZATIONS TO THE 2D POTTS MODEL

In a 2D Potts model each random variable takes on values in $\mathcal{X} = \{0, 1, \dots, q-1\}$, where q is an integer satisfying $q \geq 2$. The energy of a configuration \mathbf{x} is given by the Hamiltonian

$$\mathcal{H}(\mathbf{x}) = - \sum_{(k,\ell) \in \mathcal{B}} J_{k,\ell} \cdot [x_k = x_\ell] - \sum_{m=1}^N H_m \cdot [x_m = 0] \quad (22)$$

Here, the real coupling parameter $J_{k,\ell}$ controls the strength of the interaction between adjacent variables (x_k, x_ℓ) and the

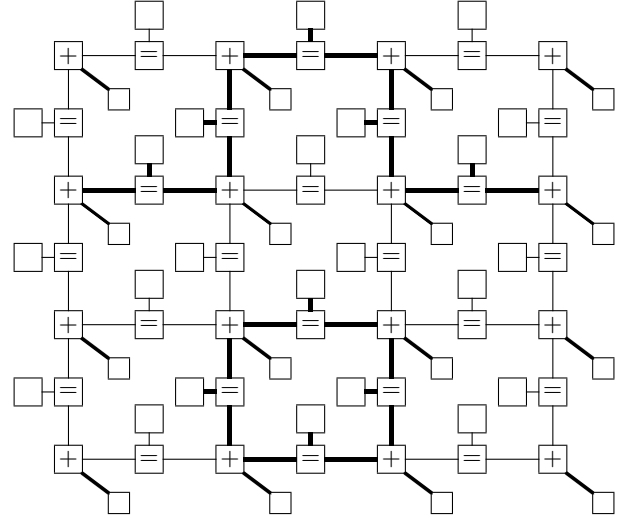


Fig. 5. Another example of a partitioning of variables on the dual Forney factor graph. The thick edges represent variables in $\tilde{\mathbf{X}}_A$, and the rest of the edges represent variables in $\tilde{\mathbf{X}}_B$. As in Figs. 3 and 4, variables in $\tilde{\mathbf{X}}_B$ are linear combinations (involving XOR factors) of the variables in $\tilde{\mathbf{X}}_A$.

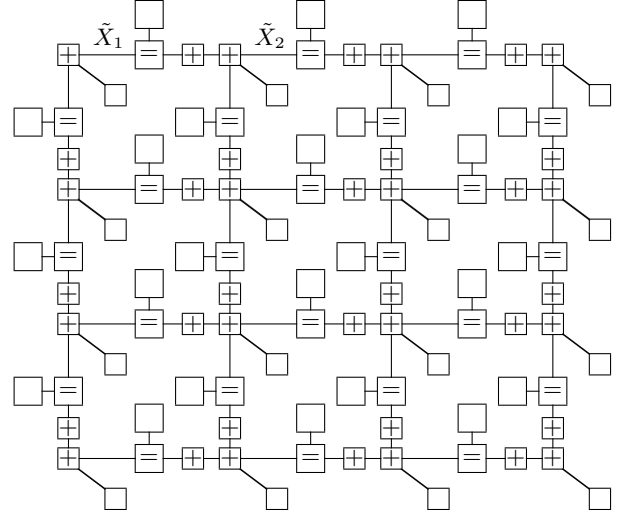


Fig. 6. The modified dual Forney factor graph of the 2D Potts model in an external field. The small boxes represent factors as in (24), the unlabeled normal-size boxes represent factors as in (23), and boxes containing + symbols represent XOR factors as in (8), where \oplus denotes addition in $\text{GF}(q)$.

real parameter H_m corresponds to the presence of an external magnetic field.

Following [2], we can obtain the (modified) dual Forney factor graph of the 2D Potts model in an external field as in Fig. 6, where the unlabeled normal-size boxes represent factors as

$$\gamma_k(\tilde{x}_k) = \begin{cases} q(e^{J_k} + q - 1), & \text{if } \tilde{x}_k = 0 \\ q(e^{J_k} - 1), & \text{otherwise,} \end{cases} \quad (23)$$

and the unlabeled small boxes have the following form

$$\lambda_m(\tilde{x}_m) = \begin{cases} e^{H_m} + q - 1, & \text{if } \tilde{x}_m = 0 \\ e^{H_m} - 1, & \text{otherwise.} \end{cases} \quad (24)$$

In this paper, we only consider ferromagnetic Potts models

in a positive external field, characterized by $J_k > 0$ and $H_m > 0$, respectively. Therefore, all the factors as in (23) and (24) will be positive.

To design importance sampling algorithms for the 2D Potts model, we need the following lemma.

Lemma 2. If $\tilde{\mathbf{x}}$ is a valid configuration in the dual Forney factor graph of the 2D Potts model, then

$$\sum_{m=1}^N \tilde{y}_m \equiv 0 \pmod{q} \quad (25)$$

Again, to draw the $\tilde{\mathbf{z}}^{(\ell)}$ -part, we can apply the following subroutine.

```

draw  $u_1^{(\ell)}, u_2^{(\ell)}, \dots, u_{|\mathcal{B}_A|}^{(\ell)} \stackrel{\text{i.i.d.}}{\sim} \mathcal{U}[0, 1]$ 
for  $k = 1$  to  $|\mathcal{B}_A|$ 
  if  $u_k^{(\ell)} < \frac{1 + (q-1)e^{-J_k}}{q}$ 
     $\tilde{z}_k^{(\ell)} = 0$ 
  else
    draw  $\tilde{z}_k^{(\ell)}$  randomly from  $\{1, 2, \dots, q-1\}$ 
  end if
end for

Here,  $(1 + (q-1)e^{-J_k})/q$  is equal to  $\gamma_k(0)/\sum_{t=1}^{q-1} \gamma_k(t)$ .
To draw the  $\tilde{\mathbf{y}}^{(\ell)}$ -part, we can apply the following.

draw  $u_1^{(\ell)}, u_2^{(\ell)}, \dots, u_{N-1}^{(\ell)} \stackrel{\text{i.i.d.}}{\sim} \mathcal{U}[0, 1]$ 
for  $m = 1$  to  $N-1$ 
  if  $u_m^{(\ell)} < \frac{1 + (q-1)e^{-H_m}}{q}$ 
     $\tilde{y}_m^{(\ell)} = 0$ 
  else
    draw  $\tilde{y}_m^{(\ell)}$  randomly from  $\{1, 2, \dots, q-1\}$ 
  end if
end for

set  $\tilde{y}_N^{(\ell)} = \sum_{m=1}^{N-1} \tilde{y}_m^{(\ell)} \pmod{q}$ 

```

Here, $(1 + (q-1)e^{-H_m})/q$ is equal to $\lambda_m(0)/\sum_{t=1}^{q-1} \lambda_m(t)$. Setting $\tilde{y}_N^{(\ell)}$ is done according to (25).

After generating $\tilde{\mathbf{x}}_A^{(\ell)} = (\tilde{\mathbf{y}}^{(\ell)}, \tilde{\mathbf{z}}^{(\ell)})$, we will update $\tilde{\mathbf{x}}_B^{(\ell)}$ to create a valid configuration $\tilde{\mathbf{x}}^{(\ell)} = (\tilde{\mathbf{x}}_A^{(\ell)}, \tilde{\mathbf{x}}_B^{(\ell)})$. The samples are used in the importance sampling scheme to estimate Z_d .

VI. NUMERICAL EXPERIMENTS

The importance sampling schemes of Section IV are applied to estimate the free energy (3) per site, i.e., $\frac{1}{N} \ln Z$, of 2D Ising models of size $N = 30 \times 30$. All simulation results show $\frac{1}{N} \ln Z$ vs. the number of samples for models with periodic boundary conditions, where to create periodic boundary conditions extra edges (with appropriate factors) are added to connect the sites on opposite sides of the boundary. In this case, $|\mathcal{B}| = 2N$.

We consider 2D ferromagnetic Ising models in an external field with spatially varying model parameters in Section VI-A,

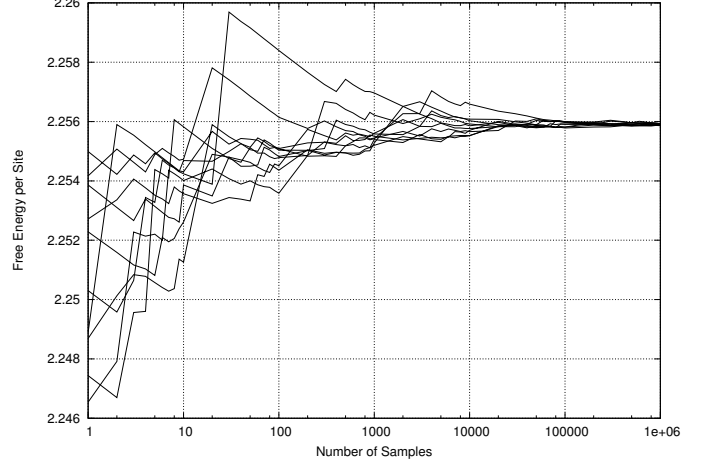


Fig. 7. Estimated free energy per site vs. the number of samples for a 30×30 ferromagnetic Ising model in an external field with periodic boundary conditions, where $J_k \sim \mathcal{U}[0.1, 1.0]$ for $k \in \mathcal{B}_A$, $J_k \sim \mathcal{U}[1.15, 1.25]$ for $k \in \mathcal{B}_B$, and $H_m \sim \mathcal{U}[0.2, 0.8]$. The plot shows ten different sample paths obtained from Algorithm 2 on the dual factor graph.

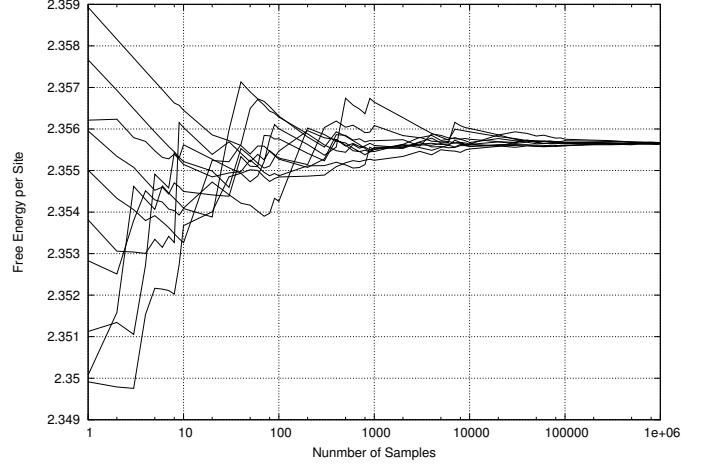


Fig. 8. Everything as in Fig. 7, but with $J_k \sim \mathcal{U}[1.25, 1.35]$ for $k \in \mathcal{B}_B$, using Algorithm 2 on the dual factor graph.

and 2D ferromagnetic Ising models with spatially varying coupling parameters in the absence of an external field in Section VI-B. We will also compare the efficiency of the importance sampling scheme and uniform sampling. This comparison was carried out for models in a strong external field in [2]. In the absence of an external field, applying Monte Carlo methods (Gibbs sampling and uniform sampling) in the dual domain to 2D Ising models is also discussed in [1], [3]. In Section VI-C, we consider 2D Potts models of size $N = 30 \times 30$ with periodic boundary conditions.

Comparisons with Gibbs sampling [24] and the Swendsen-Wang algorithm [25] are discussed in Appendix II.

A. 2D Ising models in an external field

In all the experiments, we set $J_k \stackrel{\text{i.i.d.}}{\sim} \mathcal{U}[0.1, 1.0]$ for $k \in \mathcal{B}_A$, and set $H_m \stackrel{\text{i.i.d.}}{\sim} \mathcal{U}[0.2, 0.8]$.

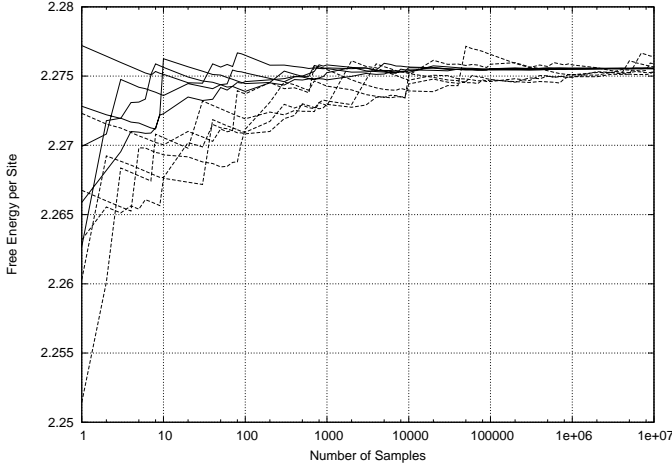


Fig. 9. Estimated free energy per site vs. the number of samples for a 30×30 ferromagnetic Ising model with periodic boundary conditions, where $J_k \sim \mathcal{U}[1.0, 1.15]$ for $k \in \mathcal{B}_A$, and $J_k \sim \mathcal{U}[1.15, 1.25]$ for $k \in \mathcal{B}_B$. The plot shows five different sample paths obtained from importance sampling (solid lines) and five different sample paths obtained from uniform sampling (dashed lines) on the dual factor graph.

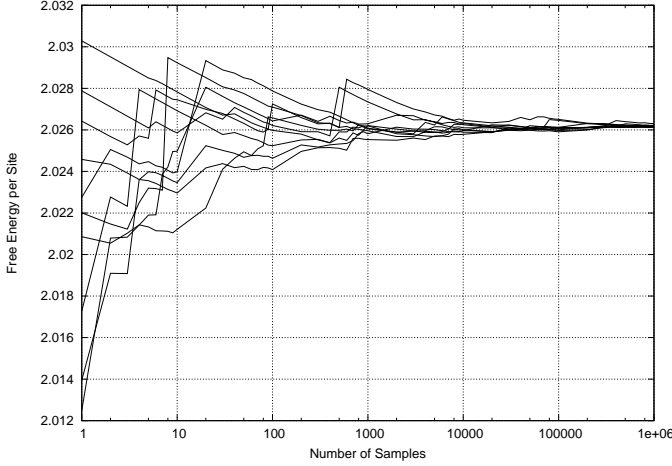


Fig. 10. Estimated free energy per site vs. the number of samples for a 30×30 ferromagnetic Ising model with periodic boundary conditions, where $J_k \sim \mathcal{U}[0.5, 1.15]$ for $k \in \mathcal{B}_A$, and $J_k \sim \mathcal{U}[1.15, 1.25]$ for $k \in \mathcal{B}_B$. The plot shows ten different sample paths obtained from importance sampling.

In the first experiment, we set $J_k \stackrel{\text{i.i.d.}}{\sim} \mathcal{U}[1.15, 1.25]$ for $k \in \mathcal{B}_B$. Simulation results for one instance of the Ising model obtained from Algorithm 2 are shown in Fig. 7, where the estimated free energy per site is about 2.255(9).

In the second experiment, $J_k \stackrel{\text{i.i.d.}}{\sim} \mathcal{U}[1.25, 1.35]$ for $k \in \mathcal{B}_B$. For one instance of the model, simulation results obtained from Algorithm 2 are shown in Fig. 8. The estimated free energy per site is about 2.3556.

B. 2D Ising models in the absence of an external field

We consider 2D Ising models in the absence of an external magnetic field, and set $J_k \stackrel{\text{i.i.d.}}{\sim} \mathcal{U}[1.15, 1.25]$ for $k \in \mathcal{B}_B$, in both experiments.

We set $J_k \stackrel{\text{i.i.d.}}{\sim} \mathcal{U}[1.0, 1.15]$ for $k \in \mathcal{B}_A$, in the first

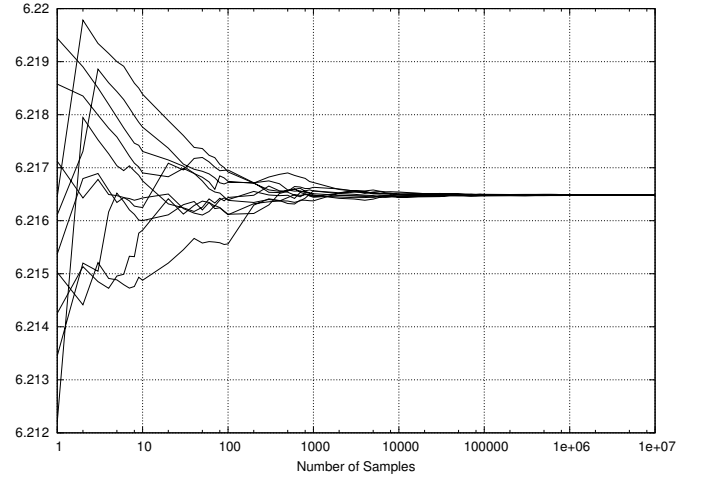


Fig. 11. Estimated free energy per site vs. the number of samples for a 30×30 4-state Potts model in an external field, and with periodic boundary conditions, with $J_k \sim \mathcal{U}[0.75, 2.25]$ for $k \in \mathcal{B}_A$, $J_k \sim \mathcal{U}[2.25, 3.25]$ for $k \in \mathcal{B}_B$, and $H_m \sim \mathcal{U}[0.5, 1.5]$. The plot shows ten different sample paths obtained from importance sampling in the dual factor graph.

experiment. Fig. 9 shows simulation results obtained from importance sampling (solid lines) and from uniform sampling (dashed lines) for one instance of the Ising model. From Fig. 9, the estimated free energy per site is about 2.275.

As was pointed out in [2], uniform sampling could be employed for models at very low temperature (i.e., very large J_k), however, for a wider range of model parameters, it has problems with slow and erratic convergence.

In the second experiment, we set $J_{k,\ell} \stackrel{\text{i.i.d.}}{\sim} \mathcal{U}[0.5, 1.15]$ for $k \in \mathcal{B}_A$. Fig. 10 shows simulation results obtained from importance sampling for one instance of the model. From Fig. 10, the estimated $\frac{1}{N} \ln Z$ is about 2.026.

C. 2D Potts models in an external field

In a 2D 4-state Potts model, we set $J_k \stackrel{\text{i.i.d.}}{\sim} \mathcal{U}[0.75, 2.25]$ for $k \in \mathcal{B}_A$ and $J_k \stackrel{\text{i.i.d.}}{\sim} \mathcal{U}[2.25, 3.25]$ for $k \in \mathcal{B}_B$. The external field is set to $H_m \stackrel{\text{i.i.d.}}{\sim} \mathcal{U}[0.5, 1.5]$.

Simulation results obtained from importance sampling in the dual factor graph are shown in Fig. 11 where the estimated free energy per site is about 6.2165.

D. Discussion

It is numerically advantageous to replace each factor (9) in the dual factor graph by

$$\lambda_m(\tilde{x}_m) = (\tanh H_m)^{\tilde{x}_m} \quad (26)$$

and each factor (10) by

$$\gamma_k(\tilde{x}_k) = (\tanh J_k)^{\tilde{x}_k} \quad (27)$$

The required scale factor to recover Z_d , can then be computed by multiplying all the local scale factors in terms of $\cosh J_k$ and $\cosh H_m$.

Note that $\lim_{t \rightarrow \infty} \tanh t = 1$, therefore the factors in (27) tend to constant if J_k is large for $k \in \mathcal{B}_B$, which explains the

reason for the fast convergence of the importance sampling schemes in this case. If all the model parameters (i.e., J_k and H_m) are large, (26) and (27) both tend to constant factors. In this case, uniform sampling is also expected to exhibit good convergence in the dual domain.

VII. CONCLUSION

Two importance sampling schemes were presented for estimating the partition function of the 2D ferromagnetic Ising model. Both schemes are described in the dual Forney factor graph representing the model. After introducing auxiliary importance sampling distributions, the methods operate by simulating a subset of the variables, followed by doing the computations using the remaining variables. The schemes can efficiently compute an estimate of the partition function in a wide range of model parameters. With our choices of partitioning, this is particularly the case when a subset of the coupling parameters of the model is strong. The methods of this paper should be compared to the method introduced in [2], where the emphasis is on models in a strong external field.

Depending on the value of the model parameters and their spatial distributions, different choices of partitioning yield schemes with different convergence properties. Our schemes once combined with annealed importance sampling are capable of handling more demanding cases, see Appendix I.

The schemes of this paper are applicable to the three-dimensional Ising model too; see [2] for a similar approach. For duality results in the context of statistical physics, see [5], [26], [27, Chapter 16], [28, Chapter 10].

APPENDIX I

We explain how to employ annealed importance sampling in the dual factor graph to estimate the partition function of the 2D Ising model, when J_k , for $k \in \mathcal{B}_B$ is relatively strong. For simplicity, we assume that the coupling parameters associated with the thick edges, the coupling parameters associated with the thin edges, and the external magnetic field are all constant, denoted by J_A , J_B , and H , respectively.

We thus denote the partition function by $Z_d(J_A, J_B, H)$, and express $Z_d(J_A, J_B, H)$ using a sequence of intermediate partition functions by varying J_B in V levels as

$$Z_d(J_A, J_B, H) = Z_d(J_A, J_B^{\alpha_V}, H) \prod_{v=0}^{V-1} \frac{Z_d(J_A, J_B^{\alpha_v}, H)}{Z_d(J_A, J_B^{\alpha_{v+1}}, H)} \quad (28)$$

Here, unlike typical annealing schemes used in the original domain, $(\alpha_0, \alpha_1, \dots, \alpha_V)$ is an increasing sequence, where $1 = \alpha_0 < \alpha_1 < \dots < \alpha_V$.

If α_V is large enough, $Z_d(J_A, J_B^{\alpha_V}, H)$ can be estimated efficiently via the proposed importance sampling schemes of Section IV. As for the intermediate steps, a sampling technique that leaves the target distribution invariant (e.g., Metropolis algorithms, Gibbs sampling [24]), is required at each level. These intermediate target probability distributions correspond to the intermediate partition functions.

The number of levels V should be sufficiently large to ensure that the intermediate target distributions are close enough, and estimating $Z_d(J_A, J_B^{\alpha_V}, H)$ is feasible. See [21] for more details.

APPENDIX II

We compare the performance of Monte Carlo methods in the original and in the dual factor graphs to compute the free energy per site, i.e., $\frac{1}{N} \ln Z$, of 2D Ising models in the absence of an external field and with constant coupling parameter J .

For different values of J , the convergence of Gibbs sampling [24] and the Swendsen-Wang algorithm [25] in the original factor graph, is compared to the convergence of uniform sampling and Gibbs sampling in the dual factor graph. We have considered the baseline (uniform sampling) in the dual domain. Clearly, convergence of uniform sampling can be significantly improved by applying our proposed importance sampling schemes.

Let $f : \mathcal{X}^N \rightarrow \mathbb{R}_{>0}$, where $\mathbb{R}_{>0} = \{x \in \mathbb{R} : x > 0\}$. We use the following methods to compute an estimate of the partition function as

$$Z = \sum_{\mathbf{x} \in \mathcal{X}^N} f(\mathbf{x}) \quad (29)$$

Method 1:

Suppose samples $\mathbf{x}^{(1)}, \mathbf{x}^{(2)}, \dots, \mathbf{x}^{(L)}$ are drawn uniformly and independently from \mathcal{X}^N .

Then

$$\hat{Z} = \frac{|\mathcal{X}^N|}{L} \sum_{\ell=1}^L f(\mathbf{x}^{(\ell)}) \quad (30)$$

is an unbiased estimator for Z . I.e.,

$$\mathbb{E}[\hat{Z}] = Z$$

Method 2 [29]:

Let

$$p(\mathbf{x}) = \frac{f(\mathbf{x})}{Z} \quad (31)$$

Suppose samples $\mathbf{x}^{(1)}, \mathbf{x}^{(2)}, \dots, \mathbf{x}^{(L)}$ are drawn from \mathcal{X}^N according to $p(\mathbf{x})$.

Then

$$\hat{\Gamma} = \frac{1}{L|\mathcal{X}^N|} \sum_{\ell=1}^L \frac{1}{f(\mathbf{x}^{(\ell)})} \quad (32)$$

is an unbiased estimator for $1/Z$. I.e.,

$$\mathbb{E}[\hat{\Gamma}] = 1/Z$$

In our numerical experiments, drawing samples according to $p(\mathbf{x})$ is done using Gibbs sampling or the Swendsen-Wang algorithm. These samples are then used in (32) to compute an estimate of Z .

We consider 2D Ising models of size $N = 5 \times 5$, with periodic boundary conditions. Note that, such a small value of N , allows us to compute the exact value of the free energy via direct enumeration.

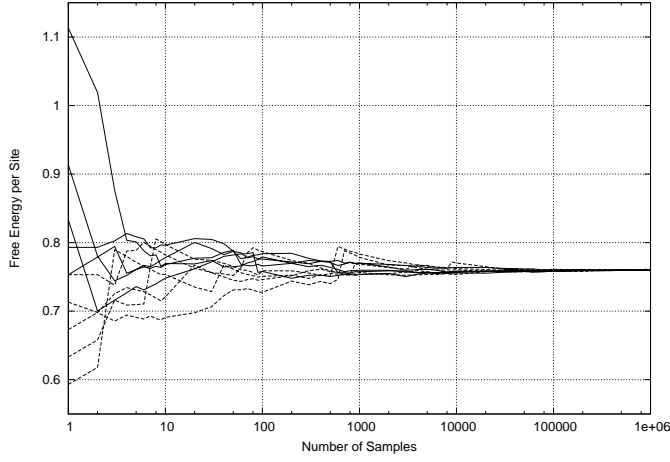


Fig. 12. Estimated free energy per site vs. the number of sample for a 5×5 Ising model with periodic boundary conditions, with $J = 0.25$. The plot shows five different sample paths obtained from the Swendsen-Wang algorithm (solid lines), and five different sample paths obtained from uniform sampling (dashed lines) in the original factor graph.

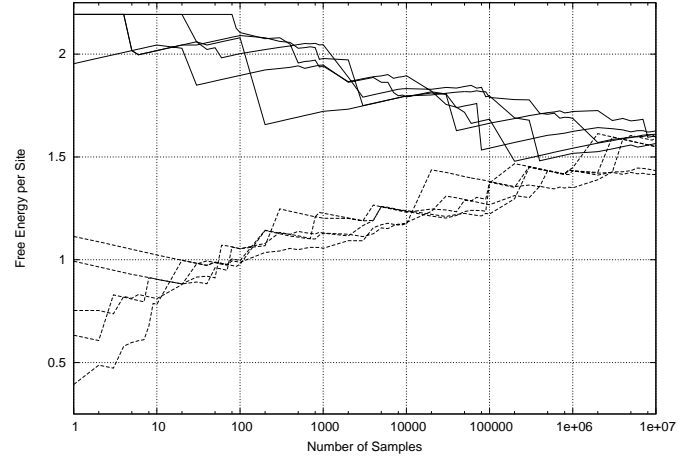


Fig. 14. Estimated free energy per site vs. the number of sample for a 5×5 Ising model with periodic boundary conditions, with $J = 0.75$. The plot shows five different sample paths obtained from the Swendsen-Wang algorithm (solid lines), and five different sample paths obtained from uniform sampling (dashed lines) in the original factor graph.

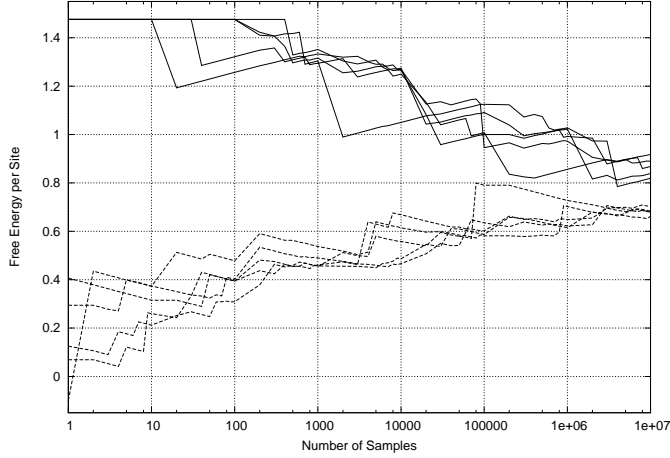


Fig. 13. Estimated free energy per site vs. the number of sample for a 5×5 Ising model with periodic boundary conditions, with $J = 0.25$. The plot shows five different sample paths obtained from Gibbs sampling (solid lines), and five different sample paths obtained from uniform sampling (dashed lines) in the dual factor graph.

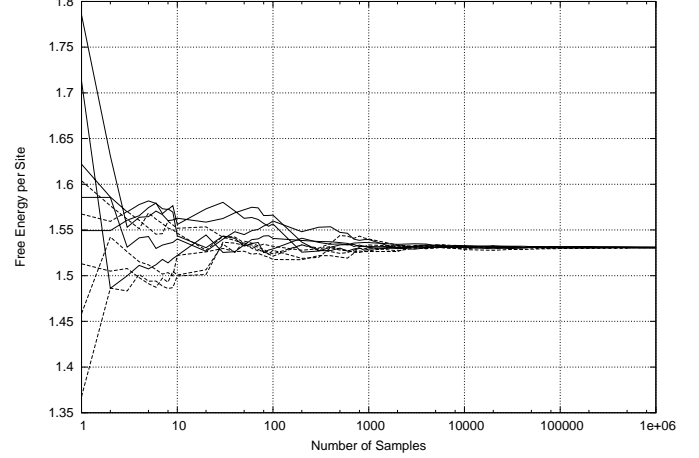


Fig. 15. Estimated free energy per site vs. the number of sample for a 5×5 Ising model with periodic boundary conditions, with $J = 0.75$. The plot shows five different sample paths obtained from Gibbs sampling (solid lines), and five different samples paths obtained from uniform sampling (dashed lines) in the dual factor graph.

In the first experiment, we set $J = 0.25$ (relatively high temperature). In this case, the exact value of the free energy per site (up to five decimal points) is 0.76006.

Fig. 12 shows simulation results obtained from the Swendsen-Wang algorithm (solid lines) and uniform sampling (dashed lines) in the original factor graph, and Fig. 13 shows simulation results obtained from Gibbs sampling (solid lines) and uniform sampling (dashed lines) in the dual factor graph.

In the second experiment, $J = 0.75$ (relatively low temperature), where the exact value of the free energy per site (up to five decimal points) is 1.53048.

Simulation results obtained from the Swendsen-Wang algorithm (solid lines) and uniform sampling (dashed lines) in the original factor graph are shown in Fig. 14. Simulation results

obtained from Gibbs sampling (dashed lines) and uniform sampling (solid lines) in the dual factor graph are shown in Fig. 15. In both cases (i.e., Gibbs sampling in the dual factor graph and the Swendsen-Wang algorithm in the original factor graph), we have used (32) to compute an estimate of Z .

At high temperature (i.e., small J), we observe faster mixing with Monte Carlo methods in the original factor graph. In sharp contrast, uniform sampling and Gibbs sampling in the dual factor graph converge extremely well at low temperature (i.e., large J), while Monte Carlo methods in the original factor graph suffer from slow convergence. Indeed, convergence of Monte Carlo methods in the dual factor graph improves as J increases.

Finally, Jerrum and Sinclair have proposed a randomized

algorithm to estimate the partition function of the 2D Ising model, which is polynomial-time for *all* temperatures [6]. Their algorithm uses the high temperature expansion of the partition function, which coincides with the dual domain representation of the Ising model in terms of Forney factor graph. However, the computational complexity of their algorithm is $O(N^3)$. Also their proposed Markov chain seems to be different from the schemes of this paper [6, Section 4]. The computational complexity of our proposed algorithms is $O(N)$ per sample, which makes the total computational complexity $O(NL)$.

ACKNOWLEDGEMENTS

The author would like to thank Hans-Andrea Loeliger and Justin Dauwels for their helpful comments. The author is grateful to Pascal Vontobel for pointing out [5] to him, and for proofreading an earlier draft of this paper.

REFERENCES

- [1] M. Molkaiaie and H.-A. Loeliger, "Partition function of the Ising model via factor graph duality," *Proc. 2013 IEEE Int. Symp. on Information Theory*, Istanbul, Turkey, July 7–12, 2013, pp. 2304–2308.
- [2] M. Molkaiaie, "An importance sampling scheme on dual factor graphs. I. models in a strong external field," [arXiv:1401.4912 \[stat.CO\]](https://arxiv.org/abs/1401.4912), 2014.
- [3] A. Al-Bashabsheh and Y. Mao, "On stochastic estimation of partition function," [arXiv:1401.7273 \[cs.IT\]](https://arxiv.org/abs/1401.7273), 2014.
- [4] K. Binder and D. W. Heermann, *Monte Carlo Simulation in Statistical Physics*. Springer, 2010.
- [5] R. Savit, "Duality in field theory and statistical systems," *Rev. of Modern Physics*, vol. 52, pp. 453–487, April 1980.
- [6] M. Jerrum and A. Sinclair, "Polynomial-time approximation algorithms for the Ising model," *SIAM J. Computing*, vol. 11, pp. 1087–1116, Oct. 1993.
- [7] D. Randall and D. Wilson, "Sampling spin configurations of an Ising system," *Proc. tenth ACM-SIAM Symp. on Discrete Algorithms*, vol. 17, pp. 959–960, Jan. 1999.
- [8] B. A. Cipra, "An introduction to the Ising model," *Amer. Mathematical Monthly*, vol. 94, pp. 937–959, Dec. 1987.
- [9] M. Niss, "History of the Lenz-Ising model 1920–1950: from ferromagnetic to cooperative phenomena," *Archive for History of Exact Sciences*, vol. 59, pp. 267–318, Springer-Verlag, March 2005.
- [10] J. M. Yeomans, *Statistical Mechanics of Phase Transitions*. Oxford University Press, 1992.
- [11] D. E. Knuth, "Two notes on notation," *Amer. Mathematical Monthly*, vol. 99, pp. 403–422, May 1992.
- [12] G. D. Forney, Jr., "Codes on graphs: normal realization," *IEEE Trans. Inform. Theory*, vol. 47, pp. 520–548, Feb. 2001.
- [13] H.-A. Loeliger, "An introduction to factor graphs," *IEEE Signal Proc. Mag.*, vol. 29, pp. 28–41, Jan. 2004.
- [14] J. M. Hammersley and D. C. Handscomb, *Monte Carlo Methods*. Methuen & Co., London, 1964.
- [15] R. M. Neal, *Probabilistic Inference Using Markov Chain Monte Carlo Methods*. Techn. Report CRG-TR-93-1, Dept. Computer Science, Univ. of Toronto, Sept. 1993.
- [16] G. D. Forney, Jr., "Codes on graphs: duality and MacWilliams identities," *IEEE Trans. Inform. Theory*, vol. 57, pp. 1382–1397, Feb. 2011.
- [17] A. Al-Bashabsheh and Y. Mao, "Normal factor graphs and holographic transformations," *IEEE Trans. Inform. Theory*, vol. 57, pp. 752–763, Feb. 2011.
- [18] G. D. Forney, Jr. and P. O. Vontobel, "Partition functions of normal factor graphs," *2011 Information Theory and Applications Workshop*, La Jolla, USA, Feb. 6–11, 2011.
- [19] R. J. Baxter, *Exactly Solved Models in Statistical Mechanics*. Dover Publications, 2007.
- [20] R. J. McEliece, *The Theory of Information and Coding: A Mathematical Framework for Communication*. Addison-Wesley, 1977.
- [21] R. M. Neal, "Annealed importance sampling," *Statistics and Computing*, vol. 11, pp. 125–139, 2001.
- [22] R. Salakhutdinov and I. Murray, "On the quantitative analysis of deep belief networks," *Proc. 25th Int. Conf. on Machine Learning*, Helsinki, Finland, July 5–9, 2008, pp. 872–879.
- [23] M. Molkaiaie and H.-A. Loeliger, "Monte Carlo algorithms for the partition function and information rates of two-dimensional channels," *IEEE Trans. Inform. Theory*, vol. 59, pp. 495–503, Jan. 2013.
- [24] S. Geman and D. Geman, "Stochastic relaxation, Gibbs distribution, and Bayesian restoration of images," *IEEE Trans. Pattern Analys. and Machine Intell.*, vol. 6, 1984, pp. 721–741.
- [25] R. H. Swendsen and J. S. Wang, "Nonuniversal critical dynamics in Monte Carlo simulations," *Phys. Rev.*, vol. 58, pp. 86–88, Jan. 1987.
- [26] H. A. Kramers and G. H. Wannier, "Statistics of the two-dimensional ferromagnet. Part I," *Phys. Rev.*, vol. 60, pp. 252–262, Aug. 1941.
- [27] G. H. Wannier, *Statistical Physics*. John Wiley, 1966.
- [28] H. Nishimoro and G. Ortiz, *Elements of Phase Transition and Critical Phenomena*. Oxford University Press, 2011.
- [29] Y. Ogata and M. Tanemura, "Estimation of interaction potentials of spatial point patterns through the maximum likelihood procedure," *Ann. Inst. Statist. Math.*, vol. 33, pp. 315–338, 1981.